

1-1-2007

## Design and analysis of general and travelling dielectrophoresis

T. Kinkeldei  
*University of Wollongong*

W.H Li  
*University of Wollongong, weihuali@uow.edu.au*

Follow this and additional works at: <https://ro.uow.edu.au/engpapers>



Part of the [Engineering Commons](#)

<https://ro.uow.edu.au/engpapers/2814>

---

### Recommended Citation

Kinkeldei, T. and Li, W.H: Design and analysis of general and travelling dielectrophoresis 2007, 346-352.  
<https://ro.uow.edu.au/engpapers/2814>

# Design and Analysis of General and Travelling Dielectrophoresis

T. Kinkeldei<sup>1,2</sup>, and W.H. Li<sup>1\*</sup>

<sup>1</sup>*School of Mechanical, Materials and Mechatronic Engineering, University of Wollongong, Wollongong, NSW 2522, Australia*

<sup>2</sup>*School of Mechanical, University of Karlsruhe, Forschungsuniversitaet Karlsruhe, Baden Wuerttemberg 76131, Germany*

---

## Abstract:

This paper presents the simulation of general and travelling dielectrophoretic forces, as well as the movement of the particles in a sandwich structure micro-device. The electrode geometry of the micro device used for simulation is an interdigitated bar electrode. The simulation method used to solve the equations is based on the least square finite difference method (LSFD). The simulation first calculates all forces acting at any place in the chamber, with these forces the trajectory of a particle can now be proposed. All of the particles parameters like radius, voltage, initial height, etc can easily be changed and the simulation can be redone. With this continuous trial we receive different behavior of the particles and examine the relevancy of the different changes made. This detailed information about the influences of the parameters on the procedure in the micro-device can be used for the development of further micro-devices.

*Keywords:* Dielectrophoresis, least square finite difference, simulation, general DEP, travelling wave

---

## 1. Introduction:

The development of micro-devices for handling particles in micrometer size and smaller, remains a challenge. Although a lot of work has been done in this research area there is still a need to focus on this topic, due to the big opportunities this research area unwraps. Different techniques have been used to handle these kinds of particles, from mechanical grippers to adhesive grippers to electrical handling devices. The latter have recently done a very good job in controlled manipulation and separation of particles especially in very small dimensions. One efficient effect used in electrical manipulation is called dielectrophoresis. DEP arises from the interaction of a non-uniform AC electrical field with the induced dipole in a micro-particle [1,2]. This interaction creates forces that can be used for its controlled manipulation. The utilization of DEP is steadily increasing. Latest research shows, that DEP Forces can be used to handle and separate carbon nanotubes [3] due to semi conducting or metallic. Other particles have also been dealt with successfully, particularly biological particles such as cells [4], viruses [5], and DNA [6] but also synthetic particles like latex spheres [7]. The different particles have different properties, which can be used to clearly identify and handle them and can be used to separate particle mixtures. Examples for these properties are different radius or different behaviour to the frequent of the applied

\* Corresponding author. Phone: +61 2 4221 3490; Fax: +61 2 4221 3101.  
E-mail address: weihuali@uow.edu.au

voltage in the device. Also, the electrical device, and especially the electrode geometry, can be used for special applications like mixer [8], filter [9], etc. The development of DEP simulation is based on the theory used to visualize the forces of the electrical field. Due to this, for different approaches different simulation methods are used. A common method to describe the DEP forces is based on FEM [10-11]. This method is also used by most commercial software, like Ansys or Maxwell, to calculate the potential distribution for different electrode geometries. Other methods used for simulation are distributed Lagrange multiplier (DLM) [12], method of moments (MoM) [13] or finite difference (FD) [14]. Electrical fields and DEP forces have been simulated for different electrode geometries like castellated electrodes [15], cage electrodes [16], interdigitated electrodes [11] and polynomial electrodes [17]. The simulated forces show close agreement with the experimental studies. Most simulation work is focused on just the calculation of the force and doesn't deal with the movement in the microdevice. An example [11] shows the behaviour of a micro particle in a device with interdigitated electrode geometry, undergoing general DEP and hydrodynamic forces.

## 2. Theoretical Background

Pohl introduced the theory of the dielectrophoretic force in 1951 [18]. It is derived from the dipole in a spherical particle induced by an AC non uniform electrical field. The derivation of both forces for gDEP and twDEP are given by the time averaged Force  $F(t)$

$$F(t) = [m(t) \nabla] E(t) \quad (1)$$

where  $m(t)$  and  $E(t)$  are the time-dependant dipole moment and electrical field. Following the derivation from Huang the dipole moment  $m_x(t)$  is taken as an example.

$$m_x(t) = 4\pi\epsilon_m r^3 E_{x0} \{ \text{Re}[f_{cm}] \cos(\omega t + \phi_x) - \text{Im}[f_{cm}] \sin(\omega t + \phi_x) \} \quad (2)$$

Here  $\phi_x$  is the phase and  $E_{x0}$  the field magnitude as spatial functions and  $\omega t$  is the frequency. The other parameters are  $\epsilon_m$  the absolute permittivity of the suspending medium,  $r$  the radius and  $f_{cm}$  the Clausius-Mossetti factor, which is given by

$$f_{cm} = \frac{\epsilon_p - \epsilon_m}{\epsilon_p + 2\epsilon_m} \quad (3)$$

In this equation  $\epsilon_p$  and  $\epsilon_m$  are the particle and suspending medium complex permittivity, defined by  $\epsilon = \epsilon - j(\sigma/\omega)$  with  $\epsilon$  as permittivity,  $\sigma$  conductivity and  $j$  as square root from -1. This factor can be positive or negative depending on the frequency and is therefore responsible for positive or negative forces. Now solving equation (1) for the x component with equation (2) and the missing moments in y and z direction we receive the solution in x direction for the DEP force time dependant and time averaged by

$$F_x(t) = m_x(t) \frac{\partial E_x(t)}{\partial x} + m_y(t) \frac{\partial E_x(t)}{\partial y} + m_z(t) \frac{\partial E_x(t)}{\partial z} \quad (4)$$

$$\langle F_x(t) \rangle = 2\pi\epsilon_m r^3 \left[ \text{Re}(f_{cm}) \frac{\partial (E_{x0}^2 + E_{y0}^2 + E_{z0}^2)}{2\partial x} + \text{Im}(f_{cm}) \left( E_{x0}^2 \frac{\partial \phi_x}{\partial x} + E_{y0}^2 \frac{\partial \phi_y}{\partial x} + E_{z0}^2 \frac{\partial \phi_z}{\partial x} \right) \right]$$

With equation (4) for every direction x,y,z we receive the total DEP force acting on a particle from non uniform electrical fields, which is the base for our simulation work.

## 3. Numerical Integration

### 3.1 Calculation of DEP forces

The numerical equations of the simulation are based on the least square finite difference method, introduced by [1]. It can be viewed as a further development of the general finite difference method GFD,

an established method to solve numerical problems. The potential distribution is satisfied with the Laplace equation

$$\frac{\partial \phi^2}{\partial x^2} + \frac{\partial \phi^2}{\partial y^2} = 0 \quad (5)$$

where  $\phi$  is potential distribution. The electrical field can be obtained by differentiating the potential. The general and travelling wave DEP forces are numerically represented as

$$\begin{aligned} F_{eDEP} &= 2\pi\epsilon_m a^3 \text{Re}[f_{CM}] \nabla (|\text{Re}[\tilde{E}]|^2 + |\text{Im}[\tilde{E}]|^2) \\ &= 2\pi\epsilon_m a^3 \text{Re}[f_{CM}] \nabla (|\nabla \phi_R|^2 + |\nabla \phi_I|^2), \end{aligned} \quad (6)$$

$$\begin{aligned} F_{mDEP} &= -2\pi\epsilon_m a^3 \text{Im}[f_{CM}] \nabla \times (E_{Rx} E_{Iy} - E_{Ry} E_{Ix}) \hat{z} \\ &= -2\pi\epsilon_m a^3 \text{Im}[f_{CM}] [-(E_{Rx,x} E_{Iy} + E_{Rx} E_{Iy,x} - E_{Ry,x} E_{Ix} - E_{Ry} E_{Ix,x}) \hat{x} \\ &\quad + (E_{Rx,y} E_{Iy} + E_{Rx} E_{Iy,y} - E_{Ry,y} E_{Ix} - E_{Ry} E_{Ix,y}) \hat{y}] \end{aligned} \quad (7)$$

### 3.2 Particle motion

The forces acting on the particle are the gravitational force, the drag force of the fluid and finally the DEP force. The two missing forces are given by

$$\begin{aligned} F_{Flow} &= 6 \cdot \pi \cdot k \cdot r \cdot \eta (\bar{v}_m - \bar{v}_p) \\ F_{Grav} &= \frac{4}{3} \pi \cdot r^3 (\rho_p - \rho_m) \cdot g \end{aligned} \quad (8)$$

The force due to the flow is constant along the x direction and just varies in y direction with a parabolic profile; the gravitational force is a constant. The basic for the movement is equation of the momentum, it is given by

$$\begin{aligned} m\ddot{x}(t) &= F_{DEP,x} + 6 \cdot \pi \cdot \eta \cdot k \cdot r \cdot (v_m - \dot{x}(t)) \\ m\ddot{y}(t) &= F_{DEP,y} - (\rho_p - \rho_m) v \cdot g - 6 \cdot \pi \cdot \eta \cdot k \cdot \dot{y}(t) \end{aligned} \quad (9)$$

## 4. Results and Discussion

### 4.1 General DEP

The parameters used are  $\text{Re}(f_{CM}) = \pm 0.5$ , medium flow rate of 487.76  $\mu\text{m/s}$  and conductivity  $\sigma_m$  of  $10^{-4}$  S/m, a dielectric constant  $\epsilon_m$  of 80 and mass density of 1  $\text{g/cm}^3$ . The particle used for simulation is a micro latex sphere with conductivity  $\sigma_p$  of  $10^{-18}$  S/m, a dielectric constant  $\epsilon_p$  of 2.5 and a mass density of 1.05  $\text{g/cm}^3$ . A relatively low gravitational force for the particle is observed, which is just relevant over long distance travel. The other preferences of the micro device like chamber height, applied voltage, particle size and others were varied and the results were used to find out more about the particle behavior in the device.

The simulation results for both negative and positive DEP with the same particle sizes are shown in Fig. 1, where the particle size is 1  $\mu\text{m}$ . The left part of Fig.1 shows negative DEP for a release Voltage of 2 Vpp, the electrodes are marked by the grid and the bold lines at the bottom of the plot. The maximum DEP forces act at the electrode edges on the particle so that the biggest gradient of the movement occurs at the electrode edges. The trajectory of the particles of various initial heights move closer together and after a certain time and distance, much longer than this device, all the particles levitate at the same height. This is due to the balance between the gravitational force and the DEP force. At a certain height above the electrode, the gravitational force gets bigger than the DEP force and the trajectory is levelling off to an

even. In the right part of Fig. 1, the trapping of the particle can be seen, with a release Voltage of 3Vpp, the electrodes are again marked with bold lines and the grid. Depending on the initial height of the particle the stopping distance varies. The maximum force in x direction, which is responsible for trapping has to overcome the force by the flow that trapping can occur.

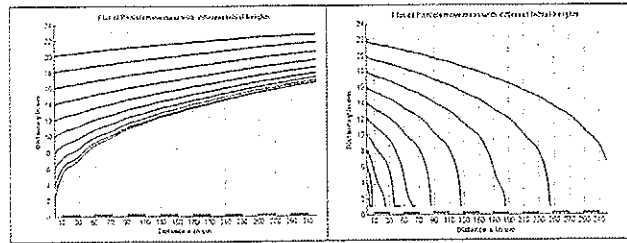


Fig. 1. Plot of particle movement for left negative DEP and right positive DEP. The chamber height is 24  $\mu\text{m}$ . The viewed Device length is 320  $\mu\text{m}$ . The electrode length and the gap between are both 20  $\mu\text{m}$

Fig. 2 shows both negative and positive DEP acting on particles with different radius. The particles start at the same initial height. For negative DEP, in the left part of Fig.2, for a Voltage of 1 Vpp and the chamber height of 20  $\mu\text{m}$ , it is received a higher levitation height for bigger radius. To see the trajectory migrating into an even the domain of the device has to be expanded. For negative DEP in the right part of Fig.2 with 3 Vpp and a chamber height of about 26  $\mu\text{m}$  the maximum stopping distance gets smaller for bigger radius.

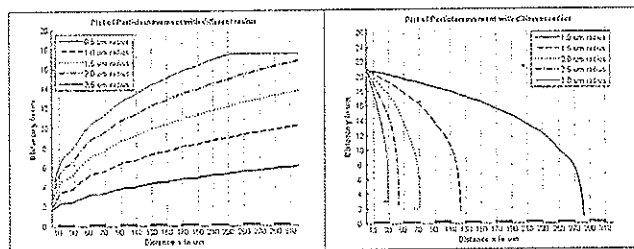


Fig. 2. Negative (left) and positive DEP for different particles sizes.

The effect of electrode geometry on both negative and positive DEPs are shown in Fig. 3. As can be seen from this figure, for an electrode width of 25  $\mu\text{m}$  we receive the highest DEP forces and for the electrode of 15  $\mu\text{m}$  the lowest forces. The reason for this is due to the potential distribution. Although there is no change at the electrode surface in x direction, there is a big change in y direction. This leads to bigger average forces in the device above the electrode and therefore to a higher levitation or earlier stopping with increasing width of the electrode. With electrode geometries of bigger width particles can be levitated higher or trapped earlier in the device.

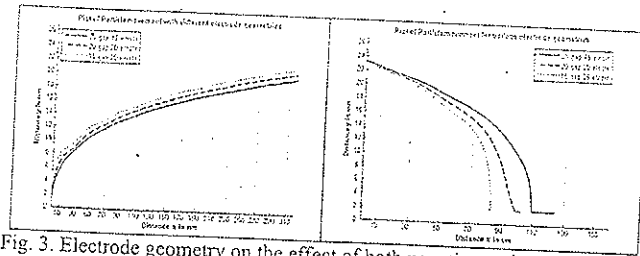


Fig. 3. Electrode geometry on the effect of both negative and positive DEPs.

4.2 Travelling Wave DEP

The DS 19 cells, with a Clausius-Mosotti factor of 0.17 for the real part and 0.45 for the imaginary part at a frequency of 1 MHz, is employed to investigate the travelling wave DEP. The density of the cells is  $1.07 \text{ g/cm}^3$ . The cell movement is shown in Fig. 4. As can be seen from this figure, the cells move in circles to a centre above the electrodes due to just traveling wave DEP at a frequency of 1 MHz and applied Voltage of 2 Vpp and a mass density of the cell changed to  $1.4 \text{ g/cm}^3$ . As reported by Li et al [1], the twDEP force in x direction acts also in higher regions of the chamber, so that even the particle at the top are moved into traveling wave direction and travel further then at lower initial heights till they get finally caught by the forces in y direction. The effect of voltages on the travelling wave is shown in Fig. 5. The left part shows the movement of the cells as similar already seen in Fig.4. The right part shows the traveling distance that the cells cover. This curve has first a slightly parabolic increase but then converts into a straight linear increase. Unlike to general DEP it can be seen that for higher Voltage the stopping distance increases. This is the effect of a higher force in direction of the traveling wave due to the increasing voltage. Whilst the vertical forces are at the one side positive and the other side negative, the closer the particle is to the electrode the more it gets levitated afterwards. This can be figured out in the increasing wave of the trajectory, from comparing the single valleys and peaks of one trajectory and the comparing of the bigger peaks at different voltages.

A special case in traveling wave DEP is the change of the radius. This leads to a cell movement as seen in Fig.6. The acting forces are just twDEP and the gravitation at a frequency of 1 MHz and 2 Vpp and a mass density for the cell of  $1.4 \text{ g/cm}^3$ . For a better verifying we combine this figure with a plot of tw- and gDEP forces acting on particle with different radius, here we have a mass density of  $1.07 \text{ g/cm}^3$ .

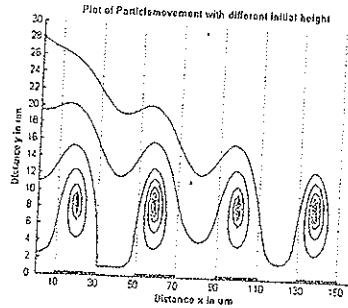


Fig. 4. The effect of the initial heights on the travelling wave particle motion.



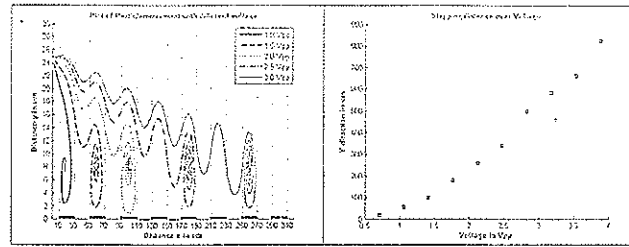


Fig. 5. The effect of voltage on the travelling wave particle motion.

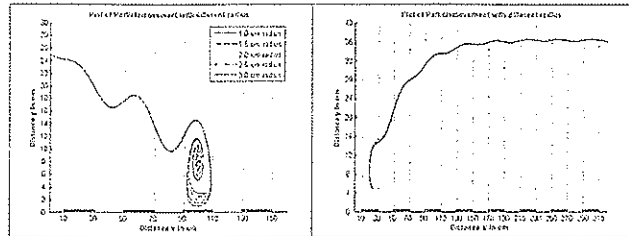


Fig. 6. Particle radius effect.

As can be seen from Fig. 6, the particle radius has no effect on the movement of the cells. The only clear thing to see is that there are different radiuses in the left plot, where the cells collide with the bottom of the chamber. In the right plot we can see a slightly thicker trajectory at the beginning over the first electrode. This little difference is due to the gDEP force, which is of more importance the closer a cell is to the electrode.

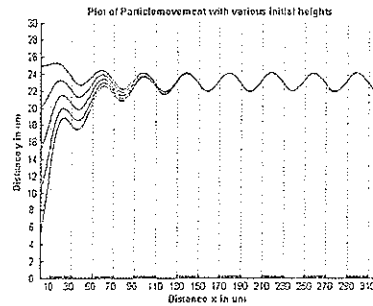


Fig. 7. The initial height effect.

Similar to the radius in a combination of tw- and gDEP the initial height has no effect on the final trajectory of the cells, as shown in Fig. 7. The difference to single twDEP is the levitation of the particle against the former trapping at the centers above the electrode. The reason for the levitation is clearly the gDEP force. As seen for negative DEP with just general DEP in the figures before, the particle are levitated to a certain height and then follow a horizontal even. It is shown that the increasing of levitation stops at a certain value and the trajectory continues instead of an even in a simple sinus oscillation due to the twDEP forces. The frequency in this plot is at 1 MHz and the Voltage is 2 Vpp, the cell size is 1 μm.

inary part at  
the cells is  
lls move in  
1 MHz and  
Li ca al [1],  
rticle at the  
ill they get  
vn in Fig. 5.  
shows the  
en converts  
ie stopping  
due to the  
gative, the  
out in the  
ry and the

as seen in  
Vpp and a  
of tw- and

## 4. Conclusion

The numerical simulation methodology was developed to study both general and traveling wave DEP based an interdigitated microelectrode array. The effects of particle size, applied voltage, initial heights on the particie motion were analysed. These simulation results are expected to optimize interdigitated microelectrodes based DEP devices.

## References

- [1] W.H. Li, H.Du, D.F.Chen, and C.Shu, "Analysis of dielectrophoretic electrode arrays for nanoparticle manipulation", *Computational Materials Science*, Vol. 30, pp. 320-325, 2004.
- [2] T. B. Jones, *Electromechanics of particles*. Cambridge; New York: Cambridge University Press, 1995.
- [3] D.F. Chen, H. Du, W.H. Li, and C. Shu, "Numerical modeling of dielectrophoresis using a meshless approach," *Journal of Micromechanics and Microengineering*, Vol. 15, pp. 1040-1048, 2005.
- [4] R. Pethig, "Dielectrophoresis: Using inhomogeneous AC electrical fields to separate and manipulate cells," *Critical Reviews in Biotechnology*, vol. 16, pp. 331-348, 1996.
- [5] M. P. Hughes, H. Morgan, F. J. Rixon, J. P. H. Burt, and R. Pethig, "Manipulation of herpes simplex virus type 1 by dielectrophoresis," *Biochimica Et Biophysica Acta-General Subjects*, vol. 1425, pp. 119-126, 1998.
- [6] M. Washizu, O. Kurosawa, I. Arai, S. Suzuki and N. Shimamoto, "Applications of Electrostatic Stretch-and-Positioning of DNA," *IEEE Transactions on Industry Applications*, vol. 31, pp. 447-456, 1995.
- [7] N. S. Green, "Dielectrophoretic separation of nano-particles," *Journal of Applied Physics*; vol. 30, 1997, pp. 41-44
- [8] J. Deval, "A Dielectrophoretic Chaotic Mixer," *IEEE*; vol. 2, 2002
- [9] H. Li, "Characterization and Modeling of a Microfluidic Dielectrophoresis Filter for Biological Species," *Journal of Microelectromechanical Systems*, vol. 14, no. 1, 2005
- [10] H. Morgan, "Numerical solution of the dielectrophoretic and travelling wave forces for interdigitated electrode arrays using the finite element method," *Journal of Electrostatics*, vol. 56, pp. 235-254, 2002.
- [11] H. Li, "On the Design and Optimization of Micro-Fluidic Dielectrophoretic Devices: A Dynamic Simulation Study," *Biomedical Microdevices*, vol. 6, pp.289-295, 2004.
- [12] A. T. J. Kadaksham, "Dielectrophoresis of nanoparticle", *Electrophoresis*, vol. 24, pp. 3625-2632, 2004.
- [13] M. P. Hughes, "Simulation of Travelling Electric Field Manipulation of Particle", pp. 48-52
- [14] B. Malnar, "Separation of latex spheres using dielectrophoresis and fluid flow", *IEEE*, vol. 150, pp. 66-69, 2003.
- [15] N. G. Green, "Ac electrokinetics: a survey of sub-micrometre particle dynamics", *J. Phys. D Appl. Phys.*, vol. 33, pp. 632-641, 2000.
- [16] J. Suehiro, "The dielectrophoretic movement and positioning of a biological cell using a three-dimensional grid electrode system", *J. Phys. D Appl. Phys.*, vol. 31, pp. 3298-3305, 1998.
- [17] Y Huang, "Electrode design for negative dielectrophoresis", *Meas. Sci. Technol.*, vol. 2, pp. 1142-1146, 1991.
- [18] H. Pohl, *The Behavior of Neutral Matter in Nonuniform Electric Fields*; Cambridge University Press: Cambridge, 1978.



